

# Semiclassical echo dynamics in the Sachdev-Ye-Kitaev model

Markus Schmitt,<sup>1,2,\*</sup> Dries Sels,<sup>3,4,5</sup> Stefan Kehrein,<sup>1</sup> and Anatoli Polkovnikov<sup>3</sup>

<sup>1</sup>*Institute for Theoretical Physics, Georg-August-Universität Göttingen,  
Friedrich-Hund-Platz 1, 37077 Göttingen, Germany*

<sup>2</sup>*Max Planck Institute for the Physics of Complex Systems, Nöthnitzer Straße 38, 01187 Dresden, Germany*

<sup>3</sup>*Department of Physics, Boston University, 590 Commonwealth Ave., Boston, MA 02215, USA*

<sup>4</sup>*Harvard University, 17 Oxford Street, Cambridge, MA 02138, USA*

<sup>5</sup>*Theory of quantum and complex system, Universiteit Antwerpen, Universiteitsplein 1, Antwerpen, BE*  
(Dated: September 13, 2022)

The existence of a quantum butterfly effect in the form of exponential sensitivity to small perturbations has been under debate for a long time. Lately, this question gained increased interest due to the proposal to probe chaotic dynamics and scrambling using out-of-time-order correlators. In this work we study echo dynamics in the Sachdev-Ye-Kitaev model under effective time reversal in a semiclassical approach. We demonstrate that small imperfections introduced in the time-reversal procedure result in an exponential divergence from the perfect echo, which allows to identify a Lyapunov exponent  $\lambda_L$ . In particular, we find that  $\lambda_L$  is twice the Lyapunov exponent of the semiclassical equations of motion. This behavior is attributed to the growth of an out-of-time-order double commutator that resembles an out-of-time-order correlator.

*Introduction.* The question of chaos and the possibility of a butterfly effect in quantum systems is a long-standing problem that received increased attention in recent years. In studies addressing the information paradox of black holes so-called out-of-time-order correlators (OTOCs) of the form

$$\langle \hat{V}(0)^\dagger \hat{W}(t)^\dagger \hat{V}(0) \hat{W}(t) \rangle_\beta \quad (1)$$

were introduced to probe the sensitivity of the dynamics to small perturbations and scrambling, i.e. the delocalization of initially local information [1–4]. A semiclassical analysis of the OTOC motivates that it can exhibit exponential growth, allowing to identify a Lyapunov exponent [5]. In fact, it was found that in a black hole theory OTOCs grow exponentially with the maximal possible rate  $\lambda_L = \frac{2\pi}{\beta}$  [6]. Remarkably, there exists a solvable model of interacting fermions, which also saturates this bound at low temperatures, namely the Sachdev-Ye-Kitaev (SYK) model [7, 8], which is a variant of a model originally introduced by Sachdev and Ye [9, 10].

OTOCs as dynamical probe of chaos and scrambling are also of interest in condensed matter systems beyond the AdS/CFT paradigm [11–17]. Particularly intriguing is the connection to the question how and in what sense closed quantum many-body systems thermalize when initially prepared far from equilibrium, which has been studied with great efforts in recent years [18, 19]. The corresponding statistical description of the stationary state is only justified if the information about the initial state cannot be recovered in practice, i.e., the dynamics is irreversible.

To assess the irreversibility of the dynamics a common approach is to study imperfect effective time reversal. In classical systems it is understood that the exponential sensitivity of the dynamics to small perturbations prohibits recovery of the initial state, because perfect time

reversal is impossible in practice [20–23]. Under chaotic dynamics any imperfection occurring in the time reversal operation leads to an exponential divergence from accurate recovery of the initial state with a rate that is largely independent of the perturbation, namely the Lyapunov exponent. This renders the improvement of the protocol prohibitively expensive.

Analogous approaches have been seized considering quantum systems. In few-body systems the decay characteristics of the Loschmidt echo  $\mathcal{L}(\tau) = |\langle \psi_0 | \hat{U}_E^\epsilon(\tau) | \psi_0 \rangle|^2$  with the echo operator  $\hat{U}_E^\epsilon(\tau) = e^{i(\hat{H} + \epsilon \hat{V})\tau} e^{-i\hat{H}\tau}$ , where  $\epsilon \hat{V}$  constitutes a small perturbation to the Hamiltonian, were used as indicator of chaos and irreversibility [24–26]. For many-body systems, however, overlaps lack experimental significance. Instead, the decay of observable echos under imperfect effective time reversal was studied to investigate irreversibility [27–31].

In the works mentioned above the focus was on decay laws occurring in the echo dynamics at late times. By contrast, imperfect effective time reversal in classical systems features initial dynamics that is governed by the butterfly effect. The possibility of a butterfly effect that occurs analogously in quantum systems is currently under debate [11, 27, 32–34]. Moreover, the realization of effective time reversal was recently reported from an experiment with trapped ions, where OTOCs were measured in the form of echo dynamics [35].

In this work we study the dynamics of the SYK model under imperfect effective time reversal in a semiclassical approach. We demonstrate that the small imperfection leads to an exponential divergence from the perfect echo. This divergence can be attributed to the exponential growth of an out-of-time-order double commutator similar to an OTOC and it allows to identify a Lyapunov exponent based on the echo dynamics.

*Imperfect effective time reversal.* In the following we will investigate the echo dynamics of an observable  $\hat{O}$  under imperfect effective time reversal. The perturbation is introduced by the action of a perturbation operator  $\hat{P}_\epsilon$  on the time-evolved state at the point of time reversal. Here  $\epsilon$  denotes a parameter for the smallness of the perturbation. A natural choice for the perturbation operator is unitary time evolution for a short interval  $\delta t$  with a perturbation Hamiltonian  $\hat{H}_p$ , i.e.,  $\hat{P}_{\delta t} = e^{-i\hat{H}_p \delta t}$ . The quantity of interest is the echo signal

$$E_{\hat{O}}(\tau) = \langle \psi_0 | \hat{U}_E^{\delta t}(\tau)^\dagger \hat{O} \hat{U}_E^{\delta t}(\tau) | \psi_0 \rangle \quad (2)$$

with the echo operator  $\hat{U}_E^{\delta t}(\tau) = e^{i\hat{H}\tau} \hat{P}_{\delta t} e^{-i\hat{H}\tau}$ . Note that in the case that the initial state is an eigenstate of the observable,  $(\hat{O} - \mu) |\psi_0\rangle = 0$ ,  $E_{\hat{O}}(\tau)$  constitutes an OTOC [31, 35]. Moreover, expanding the echo operator  $\hat{U}_E^{\delta t}(\tau)$  in orders of  $\delta t$  yields

$$\begin{aligned} \Delta E_{\hat{O}}(\tau) &= \langle \psi_0 | \hat{O} | \psi_0 \rangle - E_{\hat{O}}(\tau) \\ &= i\delta t \langle \psi_0 | [\hat{H}_p(\tau), \hat{O}] | \psi_0 \rangle \\ &\quad + \frac{\delta t^2}{2} \langle \psi_0 | [\hat{H}_p(\tau), [\hat{H}_p(\tau), \hat{O}]] | \psi_0 \rangle + \mathcal{O}(\delta t^3) \end{aligned} \quad (3)$$

for the divergence from the perfect echo. In this expression the linear term corresponds to linear response and it vanishes in the case that the initial state is an eigenstate of the observable. Hence, the quadratic term constitutes the leading contribution to the divergence from the perfect echo, accounting for the sensitivity of the dynamics to small perturbations. Using the example of the SYK Hamiltonian we will demonstrate in the following that the double commutator occurring in the quadratic term in fact determines the initial decay of the echo and that the corresponding divergence grows exponentially in time, which allows to identify a Lyapunov exponent.

*Model Hamiltonian.* The Hamiltonian of the fermionic SYK model is given by

$$\hat{H} = \frac{1}{(2N)^{3/2}} \sum_{ijkl} J_{ij;kl} \hat{c}_i^\dagger \hat{c}_j^\dagger \hat{c}_k \hat{c}_l, \quad (4)$$

where the  $J_{ij;kl}$  are complex-valued Gaussian random couplings with vanishing mean and variance  $\sigma^2 = |J_{ij;kl}|^2$ .  $N$  denotes the number of fermionic modes. The SYK model has a number of remarkable properties. Although strongly interacting, it is exactly solvable in the limit of large  $N$ . At low temperatures it exhibits an emergent conformal symmetry indicating the existence of a holographic dual [8]. It is maximally chaotic in the sense that the Lyapunov exponent occurring in OTOCs saturates the bound that was derived in for AdS black holes [6].

*Semiclassical dynamics in the SYK model.* The Truncated Wigner Approximation (TWA) constitutes an established formalism to study dynamics in the semiclassical limit by introducing a phase-space representation of

quantum operators that incorporates the defining commutation relations [36]. This approach is applicable to fermionic systems if the fermionic bilinears, which for  $N$  fermionic modes satisfy the commutation relations of  $so(2N)$ , are considered as the basic operators [37, 38].

The Weyl symbols of the fermionic bilinears are  $\tau_{\alpha\beta} = (\hat{c}_\alpha \hat{c}_\beta)_W = -(\hat{c}_\alpha^\dagger \hat{c}_\beta^\dagger)_W^*$  and  $\rho_{\alpha\beta} = \frac{1}{2}(\hat{c}_\alpha^\dagger \hat{c}_\beta - \hat{c}_\beta \hat{c}_\alpha^\dagger)_W$ . However, the substitution with these fermionic bilinears is ambiguous in the SYK Hamiltonian [39]. In a previous work it turned out that the TWA yields accurate results for the dynamics if the Hamiltonian is expressed in terms of pairing operators  $\hat{c}_\alpha \hat{c}_\beta$  and  $\hat{c}_\alpha^\dagger \hat{c}_\beta^\dagger$  [37]. The corresponding Weyl symbol is

$$\begin{aligned} \mathcal{H} = \frac{1}{(2N)^{3/2}} \sum_{ijkl} J_{ij;kl} &\left( \tau_{ji}^* \tau_{kl} + \frac{1}{2} \rho_{jk} \delta_{il} - \frac{1}{2} \rho_{jl} \delta_{ik} \right. \\ &\left. + \frac{1}{2} \rho_{il} \delta_{kj} - \frac{1}{2} \rho_{ik} \delta_{jl} \right), \end{aligned} \quad (5)$$

which yields the TWA equations of motion given in the appendix.

In the following we will consider uncorrelated initial states that are fully characterized by orbital occupation numbers  $n_\alpha = \langle \hat{c}_\alpha^\dagger \hat{c}_\alpha \rangle$ . In that case the Wigner function is well approximated by a multivariate Gaussian distribution fixed by the first and second moments [38]. We will be interested in the expansion dynamics starting from an initially imbalanced occupation similar to the situations studied in different recent cold atom experiments [40–42]. Given this initial state a suited observable to consider in the view of echo dynamics is the occupation imbalance  $\hat{M} = \frac{1}{N} \sum_{\alpha=1}^N (2n_\alpha^0 - 1)(2\hat{c}_\alpha^\dagger \hat{c}_\alpha - 1)$  with Weyl symbol  $\mathcal{M} = \frac{2}{N} \sum_{\alpha=1}^N (2n_\alpha^0 - 1)\rho_{\alpha\alpha}$ .

In the appendix we include data demonstrating that the dynamics computed using TWA is in good agreement with the exact dynamics. We find empirically that the accuracy of TWA improves as  $N$  is increased and the convergence is compatible with a power law as function of  $N$ ; see Fig. 5 in the appendix.

*Semiclassical echo dynamics.* For our purposes we choose the perturbation Hamiltonian  $\hat{H}_p = \sum_\alpha J_\alpha (\hat{c}_\alpha^\dagger \hat{c}_{\alpha+1} + h.c.)$  with normally distributed random couplings  $J_\alpha$  (variance  $J^2 = \overline{J_\alpha^2}$ ) and corresponding Weyl symbol  $\mathcal{H}_p = 2 \sum_\alpha J_\alpha \rho_{\alpha, \alpha+1}$ . Note that the dynamics under this Hamiltonian is captured exactly by the TWA, because it is quadratic.

In Fig. 1 we compare the result obtained from TWA with the exact dynamics for  $\Delta M(\tau)$  given in Eq. (3). The presented data includes a disorder average over 80 realizations of both the SKY and the perturbation Hamiltonian with system size  $N = 16$ . As initial state we consider an uncorrelated state, where one quarter of the sites is filled and the rest is empty. We find with both methods that the echo deviates increasingly from the initial value as the waiting time is increased and the results are in good agreement at short times. At long times,

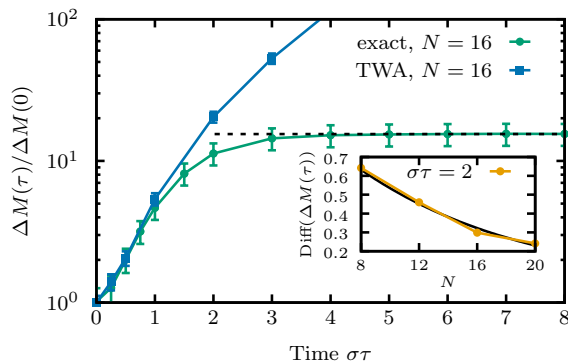


FIG. 1. Echo dynamics computed with TWA in comparison with exact results for  $J\delta t = 0.1$  and  $N = 16$  at quarter filling. The dashed line indicates the corresponding persistent echo peak height given by Eq. (15) in the appendix. The inset demonstrates that the normalized difference at the echo time is reduced as the system size is increased; the black line corresponds to an exponential fit. See appendix for further finite size analysis.

however, there is a clear discrepancy. In the result obtained from TWA the echo signal ultimately vanishes completely, meaning that  $\Delta M(\tau \rightarrow \infty) = 3/4$ . By contrast, the exact result saturates much earlier. The reason for this is that for finite  $N$  the overlap  $\langle \psi(\tau) | \hat{P}_{\delta t} | \psi(\tau) \rangle$  is non-zero, resulting in a ever-persisting revival at the echo time [31]. The corresponding saturation value can be determined in the exact simulation and it is indicated in Fig. 1 by the dashed line; see appendix for details. This persisting echo, however, vanishes for  $N \rightarrow \infty$ , because, typically, the Loschmidt echo is exponentially suppressed by the system size,  $|\langle \psi(\tau) | \hat{P}_{\delta t} | \psi(\tau) \rangle|^2 \sim e^{-Nr(\delta t)}$  with a rate function  $r(t)$ . Correspondingly, the normalized difference between exact and TWA data at the echo time,  $\text{Diff}(\Delta M(\tau))$ , is reduced when the system size is increased, as indicated in the inset of Fig. 1. In the appendix we include further data supporting the anticipated vanishing of the persistent echo in the exact dynamics for  $N \rightarrow \infty$ . This disappearing of a intrinsic difference between TWA and exact echo dynamics goes along with a generally improved accuracy of the TWA as discussed above and in the appendix. Therefore, we expect that in the limit  $N \rightarrow \infty$  results from TWA and exact dynamics will converge. Since we find in addition that the TWA result for the echo dynamics is largely independent of  $N$  (see appendix), we conclude that the TWA results obtained for finite  $N$  constitute a good approximation of the behavior in the large  $N$  limit.

With our resources for the exact dynamics, however,  $N = 20$  is the largest value we can reach due to the large number of nonvanishing matrix elements in the SYK Hamiltonian and the disorder average necessary to perform a meaningful finite size analysis. For these finite systems the persisting echo can be considered to be

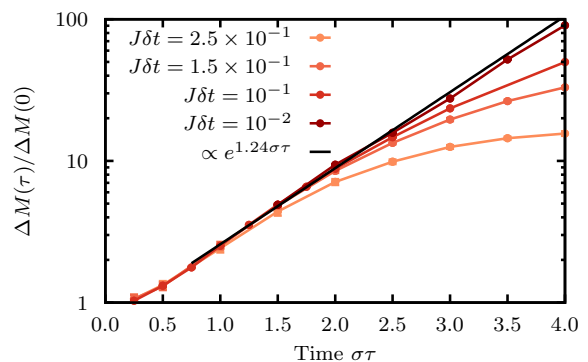


FIG. 2. TWA results for the divergence from the perfect echo computed for  $N = 20$  modes. As the perturbation strength  $\delta t$  is decreased the regime of exponential growth is extended, allowing for the identification of a Lyapunov exponent.

a genuine quantum characteristic. The TWA, applicable in the semiclassical limit, does not capture this feature, because its origin is the non-vanishing overlap between the quantum states before and after application of the perturbation operator in combination with the unitarity of quantum time evolution.

In Fig. 2 we show TWA results for the divergence from the perfect echo as defined in Eq. (3). The data exhibit a clear exponential growth of the difference to the perfect echo although the observable is bounded. We find that the parameter  $\delta t$  that determines the smallness of the perturbation controls the extent of the regime, where the exponential law is observed. In direct analogy to classical chaos the exponential divergence of the echo under imperfect effective time reversal from the perfect echo allows to identify a Lyapunov exponent  $\lambda_L$ . A fit to the data in Fig. 2 yields  $\lambda_L \approx 1.24\sigma$ . In the following we will discuss the origin of this exponential divergence in more detail.

*Role of the double commutator.* In the exact echo dynamics we observe that the quadratic term of Eq. (3), in fact, is the only relevant contribution for a large range of perturbation strengths and irrespective of the waiting time. Fig. 3a shows exact data for  $\Delta M(\tau)$  in comparison with the quadratic term  $\frac{1}{2} \langle \psi_0 | [\hat{H}_p(\tau), [\hat{H}_p(\tau), \hat{M}]] | \psi_0 \rangle \delta t^2$  as function of the perturbation strength  $\delta t$  for different waiting times  $\tau$ . Both coincide perfectly for  $J\delta t < 0.5$ .

Even though the TWA does not capture the persistent echo, Fig. 3b demonstrates that the semiclassical echo dynamics exhibit the same quadratic dependence on the perturbation strength  $\delta t$  in the regime of exponential growth. Deviations from the quadratic scaling only occur when  $\Delta M(\tau)$  begins to saturate. This supports the assertion that in Eq. (3) the second order term is the single contribution responsible for the exponential sensitivity to the imperfection in the time reversal protocol.

Similar to the OTOC (1), which is related to the square of the commutator of both operators,  $||[V, W(t)]||^2$ , ex-

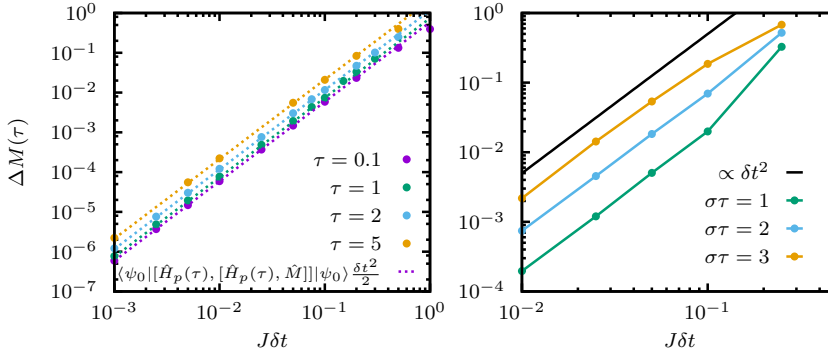


FIG. 3. Echo divergence  $\Delta M(\tau)$  for different fixed  $\tau$  as function of the perturbation strength  $\delta t$ . a) Comparison of data obtained from exact full echo dynamics (dots) with the double commutator alone (dashed lines). The double commutator appears to be the single contribution to the echo divergence over a large range of  $\tau$  and  $\delta t$ . b) Corresponding TWA result.

panding the double commutator reveals an out-of-time-order structure:

$$[\hat{H}_p(\tau), [\hat{H}_p(\tau), \hat{M}]] = \hat{H}_p(\tau)^2 \hat{M} + \hat{M} \hat{H}_p(\tau)^2 - 2\hat{H}_p(\tau) \hat{M} \hat{H}_p(\tau) \quad (6)$$

In this expression the last term accounts for the butterfly effect. For an extensive perturbation Hamiltonian  $\hat{H}_p$  the double commutator becomes extensive at late times. In the thermodynamic limit the double commutator can grow indefinitely such that it can govern the exponential divergence from the perfect echo irrespective of the higher order terms as long as  $\langle \psi_0 | [\hat{H}_p(\tau), [\hat{H}_p(\tau), \hat{M}]] | \psi_0 \rangle \delta t^2 \ll 1$ . We deduce that only at late times higher order terms become important resulting in the approach to a constant.

The inference that the double commutator governs the exponential divergence in the echo dynamics is supported by the relation to the Lyapunov exponent of the classical TWA equations, which is discussed next.

*Classical Lyapunov exponent of the TWA equations.* The Lyapunov exponent occurring in the semiclassical echo dynamics can be related to the Lyapunov exponents of the dynamical system defined by the TWA equations of motion. The classical Lyapunov exponent is defined as

$$\lambda_{cl} = \left\langle \lim_{t \rightarrow \infty} \lim_{d(\vec{x}(0), \vec{x}'(0)) \rightarrow 0} \frac{1}{t} \ln \left| \frac{d(\vec{x}(t), \vec{x}'(t))}{d(\vec{x}(0), \vec{x}'(0))} \right| \right\rangle \quad (7)$$

with coordinate vectors  $\vec{x}(t)$  and  $\vec{x}'(t)$  and  $d(\vec{x}, \vec{x}') = \sqrt{\sum_i (x_i - x'_i)^2}$  the Euclidian distance. The time-dependence of the coordinate vectors is given by the equations of motion and  $\langle \cdot \rangle$  indicates the classical average over an ensemble of trajectories.

To estimate the Lyapunov exponent of the TWA equations of motion we average the divergence of an ensemble of initially close-by trajectories on a fixed time interval;

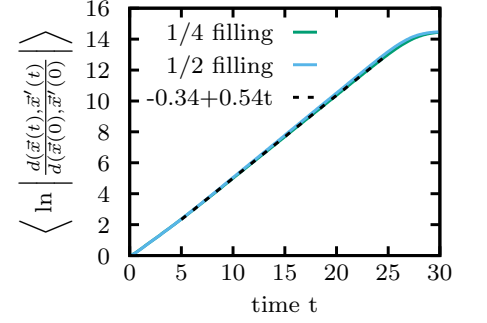


FIG. 4. Averaged divergence of initially close-by trajectories in phase space under TWA dynamics. A linear fit yields the estimate for the classical Lyapunov exponent.

details are given in the appendix. Fig. 4 displays the resulting average  $\langle \ln |d(\vec{x}(t), \vec{x}'(t))/d(\vec{x}(0), \vec{x}'(0))| \rangle$  for one realization of the SYK Hamiltonian, which we computed for half and quarter filling with  $d_0 = 10^{-8}$ . We find a clear linear dependence on time and a fit yields the classical Lyapunov exponent  $\lambda_{cl} \approx 0.54$ . The result varies only weakly as the filling is changed.

This value of  $\lambda_{cl}$  is slightly less than half of  $\lambda_L$ , which we extracted before from the echo dynamics. In the following we will argue that a factor of two between both is to be expected. We attribute the slight discrepancy to the different orders of averaging and taking the logarithm, resulting in a slightly smaller classical Lyapunov exponent as reported in Ref. [33].

The Weyl symbol of the double commutator in Eq. (6) can be written in the form

$$([\hat{H}_p(\tau), [\hat{H}_p(\tau), \hat{M}]])_W = A_j^i \frac{\partial x_i(t)}{\partial x_j(0)} + B_j^i \frac{\partial x_i(0)}{\partial x_j(t)} + C_{ij}^{kl} \frac{\partial x_k(t)}{\partial x_i(0)} \frac{\partial x_l(0)}{\partial x_j(t)} \quad (8)$$

with  $\vec{x}$  the vector of  $\rho$  and  $\tau$  coordinates of the TWA equations (cf. appendix). The modulus of all derivatives occurring in this expression grows with the classical Lyapunov exponent. However, the sums of the single derivatives in the first two terms will cancel, because they correspond to linear response. Hence, if the terms in the quadratic contribution do not cancel, at late times

$$([\hat{H}_p(\tau), [\hat{H}_p(\tau), \hat{M}]])_W \sim e^{2\lambda_{cl} t}. \quad (9)$$

The Weyl symbols of higher order commutators would contain growth rates that are higher multiples of  $\lambda_{cl}$ . Since we only observe the factor of two in the echo dynamics, we conclude that the quadratic term in Eq. (3) is in fact the one that is relevant for the butterfly effect.

*Discussion.* We found that the exponential divergence from the perfect echo in the semiclassical dynamics

is due to the growth of an out-of-time-order double commutator of the form  $[\hat{V}(\tau), [\hat{V}(\tau), \hat{W}(0)]]$ . This assertion is based on the small perturbation expansion in Eq. (3) and therefore not restricted to the semiclassical limit. In future work the structure and characteristic behavior of these objects should be further explored, in particular with regard to the sensitivity of genuine quantum dynamics far from a classical limit to small perturbations.

Regarding irreversibility our result implies that the dynamics of the SYK model is irreversible in the same sense as a chaotic classical system: Any imperfection in the time reversal procedure leads to an exponential divergence from the perfect echo and substantial improvement is prohibitively expensive, because the Lyapunov exponent is perturbation-independent.

The authors acknowledge helpful discussions with S. Davidson. This work was supported through SFB 1073 (project B03) of the Deutsche Forschungsgemeinschaft (DFG). M.S. acknowledges support by the Studienstiftung des Deutschen Volkes. D.S. acknowledges support from the FWO as post-doctoral fellow of the Research Foundation Flanders and CMTV. A.P. acknowledges support by NSF DMR-1506340 and AFOSR FA9550-16-1-0334. For the numerical computations Armadillo [46] and ITensor [47] were used.

---

\* mschmitt@pks.mpg.de

- [1] P. Hayden and J. Preskill, *Journal of High Energy Physics* **2007**, 120 (2007).
- [2] Y. Sekino and L. Susskind, *Journal of High Energy Physics* **2008**, 065 (2008).
- [3] S. H. Shenker and D. Stanford, *Journal of High Energy Physics* **2014**, 46 (2014).
- [4] A. Kitaev, “Hidden correlations in the Hawking radiation and thermal noise,” (2014), (Talk given at the Fundamental Physics Prize Symposium).
- [5] A. Larkin and Y. Ovchinnikov, *Sov. Phys. JETP* **28**, 1200 (1969).
- [6] J. Maldacena, S. H. Shenker, and D. Stanford, *Journal of High Energy Physics* **2016**, 106 (2016).
- [7] A. Kitaev, “A simple model of quantum holography,” (2015), <http://online.kitp.ucsb.edu/online/entangled15/kitaev/>; <http://online.kitp.ucsb.edu/online/entangled15/kitaev2/>.
- [8] J. Maldacena and D. Stanford, *Phys. Rev. D* **94**, 106002 (2016).
- [9] S. Sachdev and J. Ye, *Phys. Rev. Lett.* **70**, 3339 (1993).
- [10] S. Sachdev, *Phys. Rev. Lett.* **105**, 151602 (2010).
- [11] A. Bohrdt, C. B. Mendl, M. Endres, and M. Knap, *New Journal of Physics* **19**, 063001 (2017).
- [12] Y. Huang, Y.-L. Zhang, and X. Chen, *Annalen der Physik* **529**, 1600318 (2017), 1600318.
- [13] X. Chen, T. Zhou, D. A. Huse, and E. Fradkin, *Annalen der Physik* **529**, 1600332 (2017), 1600332.
- [14] E. Iyoda and T. Sagawa, *arXiv:1704.04850* (2017).
- [15] B. Swingle and D. Chowdhury, *Phys. Rev. B* **95**, 060201 (2017).
- [16] H. Shen, P. Zhang, R. Fan, and H. Zhai, *Phys. Rev. B* **96**, 054503 (2017).
- [17] A. A. Patel, D. Chowdhury, S. Sachdev, and B. Swingle, *Phys. Rev. X* **7**, 031047 (2017).
- [18] L. D’Alessio, Y. Kafri, A. Polkovnikov, and M. Rigol, *Advances in Physics* **65**, 239 (2016).
- [19] C. Gogolin and J. Eisert, *Reports on Progress in Physics* **79**, 056001 (2016).
- [20] W. Thompson, *Proceedings of the Royal Society of Edinburgh* **8**, 325 (1874).
- [21] L. Boltzmann, *Sitzungsberichte der Akademie der Wissenschaften zu Wien* **66**, 275 (1872).
- [22] J. Loschmidt, *Sitzungsberichte der Akademie der Wissenschaften zu Wien* **73**, 128 (1876).
- [23] L. Boltzmann, *Sitzungsberichte der Akademie der Wissenschaften zu Wien* **75**, 67 (1877).
- [24] A. Peres, *Phys. Rev. A* **30**, 1610 (1984).
- [25] T. Gorin, T. Prosen, T. H. Seligman, and M. Žnidarič, *Physics Reports* **435**, 33 (2006).
- [26] P. Jacquod and C. Petitjean, *Advances in Physics* **58**, 67 (2009).
- [27] B. V. Fine, T. A. Elsayed, C. M. Kropf, and A. S. de Wijn, *Phys. Rev. E* **89**, 012923 (2014).
- [28] T. A. Elsayed and B. V. Fine, *Physica Scripta* **2015**, 014011 (2015).
- [29] P. R. Zangara, D. Bendersky, and H. M. Pastawski, *Phys. Rev. A* **91**, 042112 (2015).
- [30] M. Schmitt and S. Kehrein, *EPL* **115**, 50001 (2016).
- [31] M. Schmitt and S. Kehrein, *arXiv:1711.00015* (2017).
- [32] A. E. Tarkhov, S. Wimberger, and B. V. Fine, *Phys. Rev. A* **96**, 023624 (2017).
- [33] E. B. Rozenbaum, S. Ganeshan, and V. Galitski, *Phys. Rev. Lett.* **118**, 086801 (2017).
- [34] T. Scaffidi and E. Altman, *arXiv:1711.04768*.
- [35] M. Gärttner, J. G. Bohnet, A. Safavi-Naini, M. L. Wall, J. J. Bollinger, and A. M. Rey, *Nature Physics* **13**, 781 (2017).
- [36] A. Polkovnikov, *Annals of Physics* **325**, 1790 (2010).
- [37] S. M. Davidson, D. Sels, and A. Polkovnikov, *Annals of Physics* **384**, 128 (2017).
- [38] S. M. Davidson, *Novel phase-space methods to simulate strongly-interacting many-body quantum dynamics*, Ph.D. thesis, Boston University School of Arts & Sciences (2017).
- [39] Note that this ambiguity regards the semiclassical variables. On the level of quantum operators the choices are equivalent.
- [40] U. Schneider, L. Hackermüller, J. P. Ronzheimer, S. Will, S. Braun, T. Best, I. Bloch, E. Demler, S. Mandt, D. Rasch, and A. Rosch, *Nature Physics* **8**, 213 (2012).
- [41] J.-y. Choi, S. Hild, J. Zeiher, P. Schauß, A. Rubio-Abadal, T. Yefsah, V. Khemani, D. A. Huse, I. Bloch, and C. Gross, *Science* **352**, 1547 (2016).
- [42] P. Bordia, H. Lüschen, S. Scherg, S. Gopalakrishnan, M. Knap, U. Schneider, and I. Bloch, *Phys. Rev. X* **7**, 041047 (2017).
- [43] C. von Keyserlingk, T. Rakovszky, F. Pollmann, and S. Sondhi, *arXiv:1705.08910*.
- [44] T. Rakovszky, F. Pollmann, and C. von Keyserlingk, *arXiv:1710.09827*.
- [45] V. Khemani, A. Vishwanath, and D. A. Huse, *arXiv:1710.09835*.
- [46] C. Sanderson and R. Curtin, *Journal of Open Source Software* **1** (2016), 10.21105/joss.00026.

[47] <http://www.itensor.org/>.

[48] L. G. Yaffe, Rev. Mod. Phys. **54**, 407 (1982).

### TWA equations of motion

For the phase space variables  $X_\alpha$  of operators  $\hat{X}_\alpha$  obeying the  $so(2N)$  algebra

$$[\hat{X}_\alpha, \hat{X}_\beta] = i f_{\alpha\beta\gamma} \hat{X}_\gamma \quad (10)$$

with structure constants  $f_{\alpha\beta\gamma}$  the classical equations of motion are determined by

$$\frac{dX_\alpha}{dt} = f_{\alpha\beta\gamma} \frac{\partial(\hat{H})_W}{\partial X_\beta} X_\gamma, \quad (11)$$

where  $(\hat{H})_W$  is the Weyl symbol of the Hamiltonian [37]; see also Ref. [48] for a general picture of classical representations of quantum models. For the phase space variables of the fermionic bilinears this yields

$$i \frac{d}{dt} \rho_{\alpha\beta} = \left( -\frac{\partial \mathcal{H}}{\partial \rho_{\gamma\alpha}} \rho_{\gamma\beta} + \frac{\partial \mathcal{H}}{\partial \tau_{\gamma\alpha}} \tau_{\beta\gamma} - \frac{\partial \mathcal{H}}{\partial \tau_{\alpha\gamma}} \tau_{\beta\gamma} \right) - \left( \alpha \leftrightarrow \beta \right)^*, \quad (12)$$

$$i \frac{d}{dt} \tau_{\alpha\beta} = \left( \frac{\partial \mathcal{H}}{\partial \rho_{\alpha\gamma}} \tau_{\gamma\beta} + \frac{\partial \mathcal{H}}{\partial \tau_{\gamma\alpha}^*} \rho_{\gamma\beta} - \frac{\partial \mathcal{H}}{\partial \tau_{\alpha\gamma}^*} \tau_{\gamma\beta} \right) - \left( \alpha \leftrightarrow \beta \right). \quad (13)$$

### Accuracy of the TWA

In order to assess the accuracy of the TWA we compare the result for expansion dynamics from an uncorrelated initial state, where one quarter of the modes is occupied and the rest is empty, with exact dynamics. Fig. 5 displays the corresponding time evolution of the occupation imbalance  $M(t)$  and the individual mode occupations  $n_i(t) = \langle \psi(t) | \hat{c}_i^\dagger \hat{c}_i | \psi(t) \rangle$  for  $N = 20$  and a disorder average involving 20 realizations. The dynamics computed using TWA is in good agreement with the exact dynamics. We find empirically that the accuracy of TWA improves as  $N$  is increased. As demonstrated in the inset of Fig. 5 the deviations from the exact result are compatible with a power law scaling;  $N^{-4}$  is shown as orientation.

### Finite size analysis

For finite mode number  $N$  the perturbed state will always have a nonvanishing overlap with the unperturbed state,  $|\langle \psi(\tau) | \hat{P}_{\delta t} | \psi(\tau) \rangle| > 0$ . Accordingly, we can decompose  $\hat{P}_{\delta t} | \psi(\tau) \rangle = \cos(\alpha_{\delta t}) | \psi(\tau) \rangle + \sin(\alpha_{\delta t}) | \phi \rangle$  by introducing the “orthogonal component”  $|\phi\rangle$  with  $\langle \psi(\tau) | \phi \rangle = 0$ . Considering this decomposition it becomes

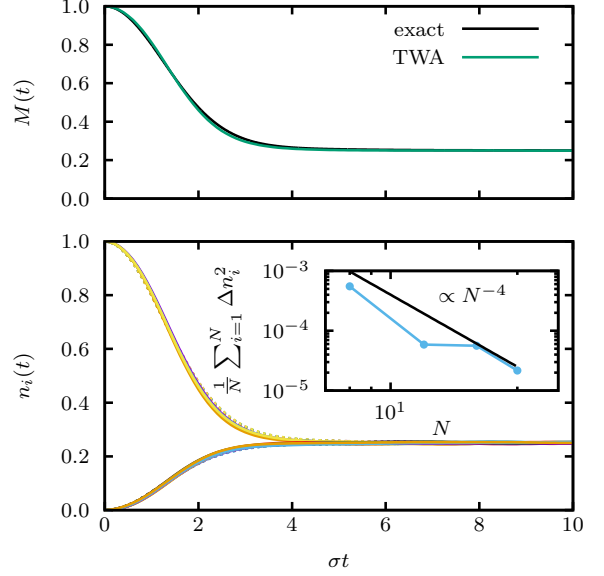


FIG. 5. Comparison of TWA results to the exact dynamics. The top panel shows the time evolution of the occupation imbalance with  $N = 20$  modes, whereas in the bottom panel the individual mode occupation numbers are shown. In the bottom panel dashed lines correspond to the exact result. The inset shows the system size dependence of the time-averaged squared deviation of the TWA from the exact result.

evident that the remaining “parallel component” of the perturbed state leads to an ever persisting echo at time  $t = 2\tau$ :

$$\begin{aligned} & \langle \psi(\tau) | \hat{P}_{\delta t}^\dagger e^{-i\hat{H}\tau} \hat{M} e^{i\hat{H}\tau} \hat{P}_{\delta t} | \psi(\tau) \rangle \\ &= \cos^2(\alpha_{\delta t}) \langle \psi_0 | \hat{M} | \psi_0 \rangle + \sin^2(\alpha_{\delta t}) \langle \phi | e^{-i\hat{H}\tau} \hat{M} e^{i\hat{H}\tau} | \phi \rangle \\ &+ \sin(2\alpha_{\delta t}) \text{Re}(\langle \psi_0 | \hat{M} e^{i\hat{H}\tau} | \phi \rangle) \end{aligned} \quad (14)$$

For finite  $N$  there is a time-independent contribution proportional to the initial value of the observable,  $\langle \psi_0 | \hat{M} | \psi_0 \rangle$ , and the overlap of the perturbed and unperturbed state,  $\cos^2(\alpha_{\delta t}) = |\langle \psi(\tau) | \hat{P}_{\delta t} | \psi(\tau) \rangle|^2$ . At late times the expectation value in the second term will attain an equilibrium value  $M_\phi^\infty = \lim_{\tau \rightarrow \infty} \langle \phi | e^{-i\hat{H}\tau} \hat{M} e^{i\hat{H}\tau} | \phi \rangle$  and the overlap in the third term will vanish. Therefore, the persistent echo peak height at large  $\tau$  is given by

$$\lim_{\tau \rightarrow \infty} E_{\hat{M}}(\tau) = \cos^2(\alpha_{\delta t}) \langle \psi_0 | \hat{M} | \psi_0 \rangle + \sin^2(\alpha_{\delta t}) M_\phi^\infty. \quad (15)$$

Exemplary results for the dynamics including effective time reversal are shown in Fig. 6. In the thermodynamic limit,  $N \rightarrow \infty$ , we will have  $\alpha_{\delta t} = \pi/2$ , i.e. the contribution given by the initial expectation value of  $\hat{M}$  vanishes and we obtain

$$\lim_{N \rightarrow \infty} \lim_{\tau \rightarrow \infty} E_{\hat{M}}(\tau) = M_\phi^\infty. \quad (16)$$



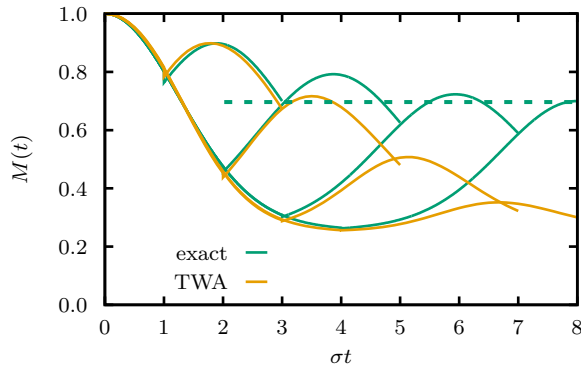


FIG. 6. Full time evolution under imperfect effective time reversal as obtained by TWA in comparison with exact dynamics for different forward times  $\tau$  with system size  $N = 20$  at quarter filling and  $J\delta t = 0.25$ . The exact dynamics show a persistent echo signal, whereas the TWA echo vanishes at long forward times. The dashed line indicates the persistent peak height as given by Eq. (15).

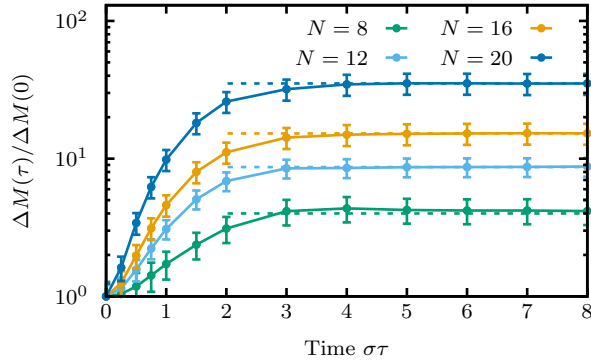


FIG. 7. Finite size analysis of exact results for the echo dynamics. The dashed lines indicate the saturation values obtained from the overlap of the perturbed with the unperturbed state. Here,  $J\delta t = 0.1$ .

In the following we present data for the variation of the echo signal  $E_M(\tau)$  with changing system sizes obtained, which supports our assertion that the persistent echo vanishes in exact quantum dynamics. For a faithful investigation of finite size effects disorder averaging is essential, because fluctuations introduced by adding new randomly coupled degrees of freedom can otherwise spoil the analysis.

In Fig. 7 we show exact results for the divergence from the perfect echo for different system sizes, including a disorder average over 80 realizations. The dashed lines indicate the saturation value of the persistent echo computed directly according to Eq. (15), where at quarter filling  $M_\phi^\infty = 1/4$ . We find very good agreement of the echo at late times with this value. As discussed in the main text and earlier in this section the saturation value increases as the system size is increased. This corresponds to the

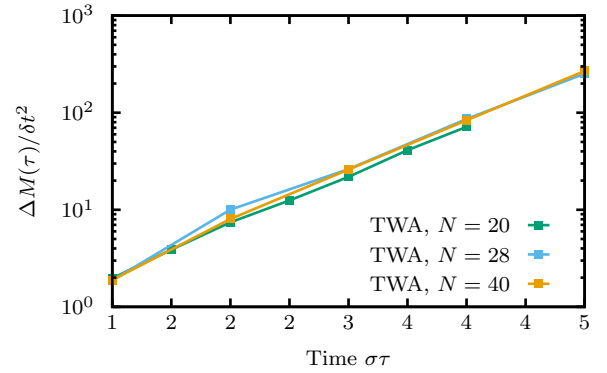


FIG. 8. Finite size analysis of results for the echo dynamics obtained from TWA.

vanishing of the persistent echo in the thermodynamic limit.

Fig. 8 displays TWA results for the divergence from the perfect echo for different system sizes. In this case we find that the results are almost identical despite a doubling of the system size.

Combining both results with the expectation that TWA becomes exact in the thermodynamic limit we conclude that the TWA result gives already at finite system sizes a good approximation of the result in the thermodynamic limit and with increasing  $N$  the exact results will converge to this.

#### Approach to determine the classical Lyapunov exponent

A common numerical method to determine the classical Lyapunov exponent

$$\lambda_{cl} = \left\langle \lim_{t \rightarrow \infty} \lim_{d(\vec{x}(0), \vec{x}'(0)) \rightarrow 0} \frac{1}{t} \ln \left| \frac{d(\vec{x}(t), \vec{x}'(t))}{d(\vec{x}(0), \vec{x}'(0))} \right| \right\rangle \quad (17)$$

is to integrate the equations of motion of two closely by initial conditions  $\vec{x}(0)$  and  $\vec{x}'(0)$  with a small fixed  $d(\vec{x}(0), \vec{x}'(0)) = d_0$  and evaluate the ratio  $d(\vec{x}(t), \vec{x}'(t))/d_0$  at a fixed time  $t$ . Then  $\vec{x}'$  is reinitialized such that  $d(\vec{x}(t), \vec{x}'(t)) = d_0$  and the equations of motion are integrated for another interval  $t$ , before the ratio of initial and final distances is evaluated again. This procedure is iterated and the samples of  $t^{-1} \ln |d(\vec{x}(t), \vec{x}'(t))/d(\vec{x}(0), \vec{x}'(0))|$  are averaged to obtain an estimate of the classical Lyapunov exponent (7).

To estimate the Lyapunov exponent of the TWA equations of motion we employed a similar approach. In this case  $\vec{x} \equiv (\rho_{\alpha,\beta}, \tau_{\alpha,\beta})$ . During a sequence of integration and reinitialization in turns we average  $\ln |d(\vec{x}(t), \vec{x}'(t))/d(\vec{x}(0), \vec{x}'(0))|$  on the whole interval  $0 < t < t_{\max}$ . Additionally, we average over many such sequences with initial conditions drawn from the Wigner



function of the initial state under consideration. In this way we obtained the result shown in Fig. 4 in the main text.

### Structure of the Weyl symbol of the double commutator

Let us denote the set of phase space variables by  $\vec{x}$ . In our case both  $H_p$  and  $M$  are linear in TWA variables,

which means that the Bopp operators take the form

$$\vec{H}_p = h(\vec{x}) + \sum_i h_i(\vec{x}) \frac{\partial}{\partial x_i} \quad (18)$$

and

$$\vec{M} = m(\vec{x}) + \sum_i m_i(\vec{x}) \frac{\partial}{\partial x_i} \quad (19)$$

where  $h(\vec{x}), h_i(\vec{x}), m(\vec{x}), m_i(\vec{x})$  are some functions of the coordinates.

---

Plugging this into the double commutator yields the Weyl symbol

$$\begin{aligned} & ([\hat{H}_p(t), [\hat{H}_p(t), \hat{M}]])_W \\ &= \left( h(\vec{x}(t)) + \sum_i h_i(\vec{x}(t)) \frac{\partial}{\partial x_i(t)} \right) \left( h(\vec{x}(t)) + \sum_j h_j(\vec{x}(t)) \frac{\partial}{\partial x_j(t)} \right) m(\vec{x}) \\ &+ \left( m(\vec{x}) + \sum_i m_i(\vec{x}) \frac{\partial}{\partial x_i} \right) \left( h(\vec{x}(t)) + \sum_j h_j(\vec{x}(t)) \frac{\partial}{\partial x_j(t)} \right) h(\vec{x}(t)) \\ &- 2 \left( h(\vec{x}(t)) + \sum_i h_i(\vec{x}(t)) \frac{\partial}{\partial x_i(t)} \right) \left( m(\vec{x}) + \sum_j m_j(\vec{x}) \frac{\partial}{\partial x_j} \right) h(\vec{x}(t)) \\ &= \sum_{ij} h_i(\vec{x}(t)) h_j(\vec{x}(t)) \frac{\partial}{\partial x_i(t)} \frac{\partial}{\partial x_j(t)} m(\vec{x}) + \sum_{ij} h_i(\vec{x}(t)) \frac{\partial h_j(\vec{x}(t))}{\partial x_i(t)} \frac{\partial}{\partial x_j(t)} m(\vec{x}) \\ &- 2 \sum_{ij} h_i(\vec{x}(t)) \frac{\partial m_j(\vec{x})}{\partial x_i(t)} \frac{\partial h(\vec{x}(t))}{\partial x_j} + \sum_{ij} m_i(\vec{x}) \frac{\partial h(\vec{x}(t))}{\partial x_j(t)} \frac{\partial}{\partial x_i} h_j(\vec{x}(t)) \\ &- \sum_{ij} m_i(\vec{x}) h_j(\vec{x}(t)) \frac{\partial}{\partial x_i} \frac{\partial h(\vec{x}(t))}{\partial x_j(t)} \end{aligned} \quad (20)$$

Now we use the chain rule  $\frac{\partial f(x_i(t_1))}{\partial x_j(t_2)} = \sum_k \frac{f(x_i(t_1))}{\partial x_k(t_1)} \frac{\partial x_k(t_1)}{\partial x_j(t_2)}$  wherever applicable, yielding

$$\begin{aligned} & ([\hat{H}_p(t), [\hat{H}_p(t), \hat{M}]])_W \\ &= \sum_{ijkl} \left( h_i(\vec{x}(t)) h_j(\vec{x}(t)) \frac{\partial^2 m(\vec{x})}{\partial x_k \partial x_l} \right) \frac{\partial x_k}{\partial x_i(t)} \frac{\partial x_l}{\partial x_j(t)} \\ &+ \sum_{jk} \left( \sum_i h_i(\vec{x}(t)) \frac{\partial h_j(\vec{x}(t))}{\partial x_i(t)} \frac{\partial m(\vec{x})}{\partial x_k} \right) \frac{\partial x_k}{\partial x_j(t)} \\ &- 2 \sum_{ijkl} \left( h_i(\vec{x}(t)) \frac{\partial m_j(\vec{x})}{\partial x_k} \frac{\partial h(\vec{x}(t))}{\partial x_l(t)} \right) \frac{\partial x_k}{\partial x_i(t)} \frac{\partial x_l(t)}{\partial x_j} \\ &+ \sum_{ik} \left( \sum_j m_i(\vec{x}) \frac{\partial h(\vec{x}(t))}{\partial x_j(t)} \frac{\partial h_j(\vec{x}(t))}{\partial x_k(t)} \right) \frac{\partial x_k(t)}{\partial x_i} \\ &- \sum_{ik} \left( \sum_j m_i(\vec{x}) h_j(\vec{x}(t)) \frac{\partial^2 h(\vec{x}(t))}{\partial x_k(t) \partial x_j(t)} \right) \frac{\partial x_k(t)}{\partial x_i} . \end{aligned} \quad (21)$$

---

Since in our case  $h(\vec{x})$  and  $m(\vec{x})$  are linear in  $\vec{x}$ , the expression can be simplified to

$$\begin{aligned} & ([\hat{H}_p(t), [\hat{H}_p(t), \hat{M}]])_W \\ &= \sum_{jk} \left( \sum_i h_i(\vec{x}(t)) \frac{\partial h_j}{\partial x_i} \frac{\partial m}{\partial x_k} \right) \frac{\partial x_k}{\partial x_j(t)} \\ &- 2 \sum_{ijkl} \left( h_i(\vec{x}(t)) \frac{\partial m_j}{\partial x_k} \frac{\partial h}{\partial x_l} \right) \frac{\partial x_k}{\partial x_i(t)} \frac{\partial x_l(t)}{\partial x_j} \\ &+ \sum_{ik} \left( \sum_j m_i(\vec{x}) \frac{\partial h}{\partial x_j} \frac{\partial h_j}{\partial x_k} \right) \frac{\partial x_k(t)}{\partial x_i} . \end{aligned} \quad (22)$$

In this form the Weyl symbol corresponds to Eq. (8) in the main text. This expression involves linear response type terms, which are linear in  $\frac{\partial x_i(t)}{\partial x_j(0)}$ , and terms that are quadratic in these derivatives. The linear terms should cancel such that they do not contribute to exponential growth; otherwise, also the response of the form  $\{\hat{H}_p(\tau)^2, \hat{M}\} = \hat{H}_p(\tau)^2 \hat{M} + \hat{M} \hat{H}_p(\tau)^2$  would grow exponentially.